567

Phase Synchrony Analysis of Network Dynamics links EEG and BOLD

Nathan Dees[1], Linda Larson-Prior[2], Tracy Nolan[2], Keara Wright[1], David Politte[2], Fred Prior[2], Sonya Bahar[1]

[1]*Center for Neurodynamics, University of Missouri-St. Louis, St. Louis MO 63121*
[2]*Mallinckrodt Institute of Radiology, Washington University Medical School, St. Louis, MO 63110*

INTRODUCTION: Cognitive function relies upon the ability of the brain to transmit and process information over distributed networks. Local field potentials, reflected in the EEG or imaged via the vascular response (BOLD fMRI) play a key role in the way in which information processing, integration and transmission are accomplished. High-frequency (>40 Hz) population activity has been proposed to primarily support local processing, while long distance interactions utilize lower frequency signaling. This is of particular interest, as recent studies using low-frequency information from the BOLD fMRI have identified known cognitive networks. While both EEG and BOLD provide important information on cognitive network behaviors, they have significantly different time scales. Phase synchronization analyses provide dynamic measures of neural activity and a natural means of integrating information between these two modalities. However, methods are required to enable to co-registration of information from both modalities in order to accurately localize those networks involved in synchronized activity. Thus we explored the feasibility of projecting current source density (CSD) derived from high density EEG (hdEEG) sources during both a behavioral (visual oddball) task and in spontaneous activity during eyes closed waking rest onto a spatial reference frame that is frequently used to display and analyze fMRI-BOLD activations (CARET (Van Essen et al., 2001)). For spontaneous activation data, such projections were compared to simultaneously acquired fMRI-BOLD data, while behavioral data were compared to fcMRI data acquired during quiet waking rest. Both data sets were also submitted to dynamic modeling to assess synchronization-based network activity.

Spatial Integration

Eight subjects participated in a 3-part visual oddball task recorded using a high-density EEG array (Compumedics Neuroscan Synamps/2™ amplifier, 64 electrodes, 1kHz sampling). Subjects sat comfortably in a sound attenuating chamber, and performed 4 runs in which they were asked to identify a target stimulus (oddball/target) under conditions where there either was or was not a distractor stimulus). EEG data were band-pass filtered (0.1-200Hz), artifact reduced using an SVD filter, epoched (-100 - 800 msec), and averaged according to stimulus type (standard, oddball, and distractor). These data were submitted to two analyses: one (Figure 1) in which CSD maps of task-related EEG activity were calculated and a second in which network dynamics based on continuous data were analyzed (Fig. 2). Four subjects participated in a simultaneous EEG/fMRI study assessing neural network activity during eyes-closed quiet wake. fMRI/BOLD data were collected (Siemens Trio 3T scanner, TR=2.2s, whole brain, 4mm^3 voxels, 15min). Simultaneous EEG was acquired using the MagLink system™ (64 channels, Compumedics Neuroscan).

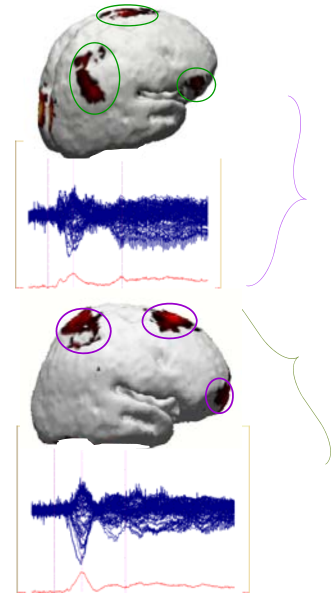

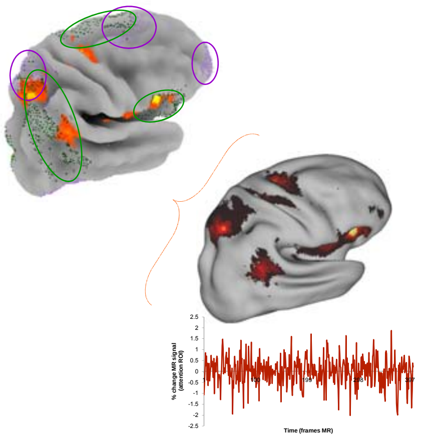

FIGURE 1: Each EEG sensor (electrode) is located relative to the brain atlas. Sensor fields are projected to the underlying cortical region. Each sensor field projects to a 6 cm² region of cortex. At **far left**, SWARM current source density localization techniques was used to overcome the coarse spatial resolution of EEG, and produce the relative P300 foci maps on Caret (**center**, purple = distractor, green = target oddball) P300 while for fcMRI anatomical images (orange, **left**, 1mm³ voxels) were combined with BOLD (4mm³ voxels) to produce images in 3mm³ Data is projected to MNI atlas space.

NEURODYNAMICS ANALYSIS: Scalp current source density (SCD) was calculated from continuous data at each electrode location using 4th order spherical splines (see Perrin et al.,1987). Data was resampled to 250 Hz and then band-pass filtered, around 6 common bands: δ (2.4 – 3.4 Hz), θ (5.4 – 6.5 Hz), low α (8 – 9 Hz), high α (9.5 – 10.5 Hz), β (19.5 – 22.5 Hz), and γ (37 – 41 Hz). The Hilbert transform of the data was taken, with signal magnitude and phase extracted prior to division of the data into epochs based on task type (standard, oddball, and distractor). Taking the Hilbert transform before dividing the data into epochs helps to avoid edge effects produced by the transform. For each stimulus type, epochs containing very-high-amplitude fluctuations or residual blink artifact were discarded. 10 regions of interest were identified for power waveform analysis based on both fMRI and EEG studies of oddball task activation, including DLPFC, FEF, M1/PMA, MT$^+$,TPJ, and lateral visual association cortices. For each ROI, the summed squared voltage for each time *t* and frequency band *b*, $\sum_{t,b} (V_{tb})^2$, was normalized for each subject and region of interest to the value $\frac{1}{N_s}\sum_s \left(\sum_{t,b} (V_{tbs})^2 \right)$ where N_s is the number of subjects included in the comparison. N_s = 6 for standard stimuli, N_s = 5 for oddball stimuli, and N_s = 3 for distractor stimuli. The mean normalized magnitude of the Hilbert transform is plotted for each bandwidth. This waveform represents an envelope of the filtered data, and can be an interpretation of power density (Doesburg et al. 2008). For synchrony analysis, a seed region was chosen on the scalp at the right TPJ, near EEG electrode CP6. Using the epoched phase values for the different bandwidths, a phase-locking value (PLV) (Lachaux et al. 1999) was calculated between the phase at this seed region and every other region on the scalp. The PLV ranges between 0 (no synchrony) and 1 (perfect synchrony), and was plotted as a topographic map for the theta, high alpha, beta, and gamma bandwidths at the exact time of the peak P300 waveform for each subject.

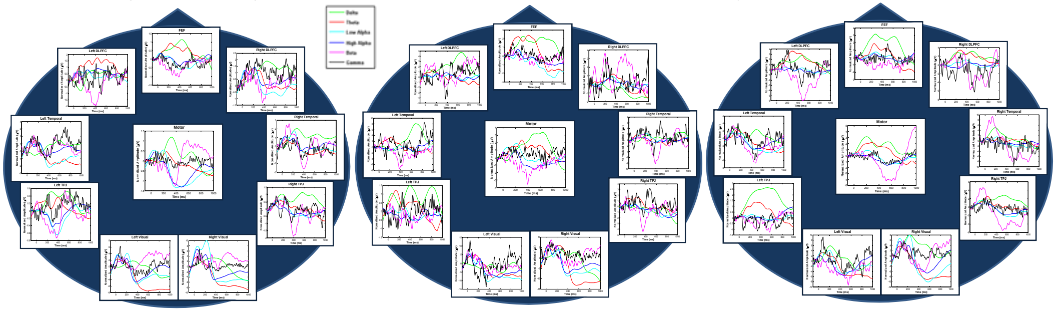

FIGURE 2: Relative amplitudes of the envelopes of band-limited data following standard (left, 6 subjects), oddball (center, 5 subjects), and distracter (right, 3 subjects) stimuli. Stimulus presentation is noted at time = 0. Plots note the multi-frequency fluctuations in all bands throughout the recording epoch.

CONCLUSIONS

Both EEG and fMRI have enhanced our understanding of the brain networks involved in the complex behaviors associated with oddball (change detection) tasks. To date, however, a functional integration of the information available from these two important techniques has not been fully accomplished. The development of fcMRI, based on the correlation structure of the BOLD time series, has indicated that persistent functional linkages exist between network elements of such important and commonly accessed systems as the attention system (dorsal and ventral, Corbetta et al., 2001). Based in part on these data, and firmly based in the literature from both modalities, we have shown the feasibility of mapping CSD-based EEG signals and fMRI BOLD to the same spatial reference space, allowing the extraction of EEG time series from ROIs known to be associated with change detection tasks such as the visual oddball task. Furthermore, those time series can then be evaluated for network synchrony/connectivity in a time frame relevant to neural processing as it is this increased temporal resolution that EEG analyses bring to the integrated EEG/fMRI analyses.

These techniques can now be moved to the more difficult task of evaluating non-task related, spontaneous activity. Our initial work in this area has focused on eyes closed waking rest, the state most commonly used in the construction of resting state BOLD functional connectivity. Early studies (see Fig. 3) showed similar patterns of connectivity in low frequency envelopes based on alpha-band activity in occipital electrode derivations (2Hz) and fcMRI evaluated using a seed region in primary visual cortex. These data need to be expanded using the techniques developed in task-related data sets under the hypothesis that a portion of the dynamics in the systems will act through regions identified as part of the default network in previous studies (Raichle et al., 2001; Fox et al., 2005).

REFERENCES

1. Perrin F, Bertrand O, Pernier J. (1987) *IEEE Trans Biomed Eng* 34:283-288.
2. Doesburg SM, Roggeveen AB, Kitajo K, Ward LM. (2007 *Cerebral Cortex* 18(2):386-396.
3. Lachaux JP, Rodriguez E, Martinerie J, Varela FJ. 1999. *Hum Brain Mapp* 8(4):194-208
4. Corbetta, M., Shulman, G.L. (2002) *Nat Rev Neurosci*, 3:201
5. Fox MD et al., (2005) *PNAS* 102:9673-9678
6. Fox MD et al. (2006) *PNAS* 103:26:10046-10051
7. Delorme A., Makeig S (2004) *J Neurosci Meth* 134:9.
8. Raichle ME et al. (2001) *PNAS* 98:676-682
9. Wagner M, Fuchs M, Kastner J (2007) *International Congress Series* 1300:185-188
10. Van Essen DC, et al.(2001) *J Am Informatics Assn*, 41:1359-1378 http://brainmap.wustl.edu/caret

FIGURE 3

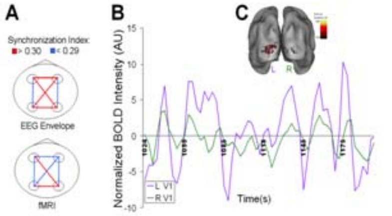

Analysis of spontaneous data acquired using simultaneous EEG/fMRI BOLD during eyes closed waking rest. The level of inter-regional synchrony is similar in EEG (2 Hz envelope, alpha band-limited data) and fcfMRI (**A**). Both modalities exhibit strong synchronization between visual regions, although EEG indicates a stronger visual to frontal linkage than is evident in the BOLD time series assessed using fcMRI (**B**, BOLD time series for L/R V1), where only cross-hemispheric correlations (**C**) reach significance (n=6, p<0.01)

FIGURE 4

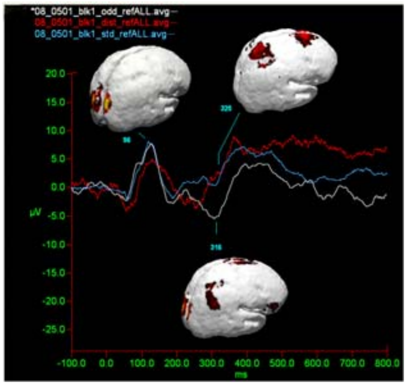

Representative data (single subject) in visual oddball task with distractor, displayed at CZ electrode. CSD projections (CURRY SWARM, 5 msec window) are displayed for time of peak activity (P100, N316 and P324) to illustrate network activity in each. Of interest is the pre-P300 activation in regions of the cortex associated with attentional switching (TPJ, N316). Examination of all data sets suggests that this region activates as brain networks switch from a poster, visuocentric response to task to more anterior, frontoparietal networks associated with decision making and motor planning.

FIGURE 5

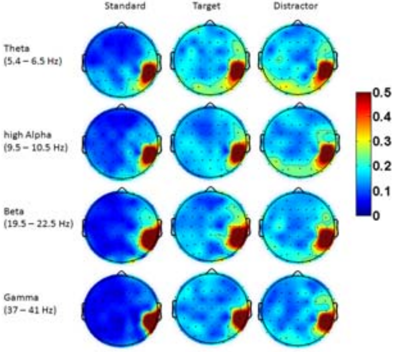

To examine the potential link between activity in TPJ (taken at electrode CP6), topographic maps of PLV at all frequencies were calculated against all other electrodes in the recording array at the instantaneous time of the peak of the P300 waveform for standard (6 subjects), oddball (5 subjects), and distractor (3 subjects) stimuli. PLVs for theta, high alpha (9.5 – 10.5 Hz), beta, and gamma bands are shown here, indicating no phase linkage in response to standard stimuli, weak linkage in theta to visual areas in both target and distractor conditions and diffuse, albeit weak, linkage in all bands to the distractor condition.

ACKNOWLEDGMENTS: The authors would like to thank Carsten Allefeld (http://www.agnld.uni-potsdam.de/~allefeld/index.html) for supplying a MATLAB script which aides in the calculation of SCD, and Donna Dierker for help mapping SWARM foci to Caret. This work was supported by the Mallinckrodt Institute of Radiology.